Spin-Crossover Materials Hot Paper

Deutsche Ausgabe: DOI: 10.1002/ange.201602441
Internationale Ausgabe: DOI: 10.1002/anie.201602441

First Step Towards a Devil's Staircase in Spin-Crossover Materials

Elzbieta Trzop[+], Daopeng Zhang[+], Lucia Piñeiro-Lopez, Francisco J. Valverde-Muñoz, M. Carmen Muñoz, Lukas Palatinus, Laurent Guerin, Hervé Cailleau, Jose Antonio Real, and Eric Collet**

Abstract: *The unprecedented bimetallic 2D coordination polymer $\{Fe[(Hg(SCN)_3)_2](4,4'\text{-bipy})_2\}_n$ exhibits a thermal high-spin (HS)↔low-spin (LS) staircase-like conversion characterized by a multi-step dependence of the HS molar fraction γ_{HS}. Between the fully HS ($\gamma_{HS}=1$) and LS ($\gamma_{HS}=0$) phases, two steps associated with different ordering appear in terms of spin-state concentration waves (SSCW). On the $\gamma_{HS}\approx 0.5$ step, a periodic SSCW forms with a HS-LS-HS-LS sequence. On the $\gamma_{HS}\approx 0.34$ step, the 4D superspace crystallography structural refinement reveals an aperiodic SSCW, with a HS-LS sequence incommensurate with the molecular lattice. The formation of these different long-range spatially ordered structures of LS and HS states during the multi-step spin-crossover is discussed within the framework of "Devil's staircase"-type transitions. Spatially modulated phases are known in various types of materials but are uniquely related to molecular HS/LS bistability in this case.*

Spin-crossover (SCO) materials are made of bistable molecules able to switch from low (LS) to high spin (HS) states (Figure 1).[1] The LS to HS thermal conversion occurs when the entropy term ($T\Delta S$), favoring the HS state, compensates the enthalpy differences (ΔH). The solely "ferro" elastic coupling, that is, favoring energetically equal states between sites with higher (HS) or lower (LS) molecular volume, can drive cooperative phase transformation from LS to HS. This is taken into account by the Ising-like model through the temperature dependent on-site effective field $h=(-\Delta H+T\Delta S)/2$. In the universal Ising phase diagram the system follows an oblique line (T, $h(T)$), determining the thermal conversion of the HS molecular fraction γ_{HS} from 0 to 1.[2] However, stepwise conversions have been reported in a vast variety of SCO materials made of Fe^{II},[3] Fe^{III},[4] Co^{II},[5] or Mn^{III}[6] ions, with the establishment of different HS-LS periodic orders on the steps. This results from competing "ferro" and "antiferro" interactions.[7]

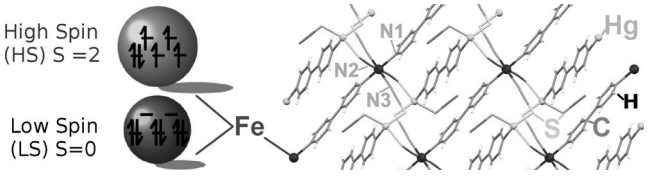

Figure 1. Electronic states of the iron ion (left) and crystal structure of the 2D metallothiocyanate Fe^{II}–Hg^{II} SCO coordination polymer.

The ANNNI model (Anisotropic Next Nearest Neighbors Interactions) is an extension of the Ising model, which explains the formation of such modulated commensurate and incommensurate structures in crystals.[8] The theoretical Devil's staircase concept was introduced to explain the rich sequence of steps that occur during the transformation of a system as the on-site field h (or T) changes (Figure 2).[9] Each step corresponds to a long-period commensurate

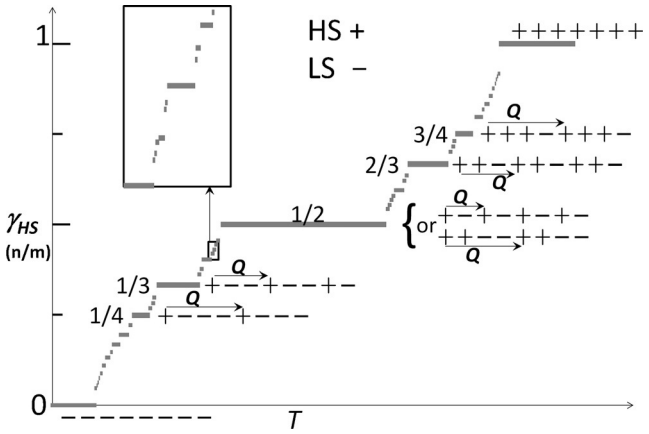

Figure 2. Theoretical Devil's staircase (modified from ref. [9d]). For SCO materials, the steps with T (or H) correspond to fractions $\gamma_{HS}=n/m$ of HS (+) molecules forming a periodic sequence with LS (−) molecules along the modulation vector Q. Structure of the simplest (thick segments) steps are represented.

[*] Dr. E. Trzop,[+] Dr. L. Guerin, Prof. H. Cailleau, Prof. E. Collet
Institut de Physique de Rennes, Université de Rennes 1
UMR UR1-CNRS 6251, 35000 Rennes (France)
E-mail: eric.collet@univ-rennes1.fr
Dr. D. Zhang,[+] Dr. L. Piñeiro-Lopez, Dr. F. J. Valverde-Muñoz, Prof. J. A. Real
Instituto de Ciencia Molecular (ICMol), Universidad de Valencia
C/ Catedrático José Beltrán Martínez 2
46980 Paterna, Valencia (Spain)
E-mail: Jose.A.Real@uv.es
Dr. D. Zhang[+]
College of Chemical Engineering, Shandong University of Technology
Zibo 255049 (China)
Prof. M. Carmen Muñoz
Departamento de Física Aplicada, Universitat Politècnica de València
Camino de Vera s/n, 46022 Valencia (Spain)
Dr. L. Palatinus
Department of Structure Analysis, Institute of Physics of Academy of Sciences of Czech Republic, 18221 Prague (Czech Republic)
[+] These authors contributed equally to this work.
Supporting information and the ORCID identification number(s) for the author(s) of this article can be found under http://dx.doi.org/10.1002/anie.201602441.

 © 2016 Wiley-VCH Verlag GmbH & Co. KGaA, Weinheim

structure, possessing a spatial modulation of states (represented by + or −) associated with a wave vector $\boldsymbol{Q}$ locked onto a rational number n/m. Between any two steps there is an infinity of steps because an infinity of rational numbers lie between any two rational numbers. For this reason such a stepped sequence of phases is called the Devil's staircase. It appears in a vast variety of systems with + or − states of different natures, including charge or spin density waves, atomic concentration waves in alloys, ferroelectric materials or spin-valve systems. Such nanostructures open up possibilities to create completely new electronic functionalities for technological applications.[10] Herein, we report the incomplete Devil's staircase during SCO of the new metallothiocyanate Fe^{II}–Hg^{II} 2D coordination polymer $\{Fe[(Hg(SCN)_3)_2](4,4'\text{-bipy})_2\}_n$ (**1**) as commensurate and incommensurate spin-state concentration waves form on the steps, with different spatial sequences of HS (+) and LS (−) states.

Self-assembly of Fe^{II}, 4,4′-bipyridine (4,4′-bipy), and $[Hg(SCN)_4]^{2-}$ in water/methanol solutions yielded **1** (Supporting Information). A fragment of the structure is shown in Figure 1. The iron sites show bistability between LS ($S=0$) and HS ($S=2$) states. Evolution of the $\chi_M T$ product (χ_M = magnetic susceptibility, T temperature) was used to characterize the conversion of γ_{HS} against T, as shown in Figure 3a. Above about 180 K, $\chi_M T \approx 3.67\ cm^3\,K\,mol^{-1}$ is practically constant and consistent with a fully Fe^{II} HS ($\gamma_{HS}=1$) phase. Below about 95 K, $\chi_M T$ is indicative of a fully Fe^{II} LS phase ($\gamma_{HS}=0$). Furthermore, the γ_{HS} versus T plot shows two other steps in addition to the HS and LS phases. One in the 108–125 K interval, where $\gamma_{HS}\approx 0.5$, and one in the 96–108 K interval around $\gamma_{HS}\approx 0.34$. Single-crystal X-ray diffraction data have been recorded for different temperatures[11] (Supporting Information) and the unit cell volume evolution confirms the steps observed in the magnetic measurement (Figure 3b). The HS structure (220 K; Supporting Information, Table S1) is triclinic $P\bar{1}$ and consists of slightly distorted centrosymmetric octahedral $Fe^{II}N_6$ sites, axially connected by 4,4′-bipy ligands (through N1; Figure 1). The equatorial positions are occupied by the N2 and N3 atoms of two crystallographically unique NCS-groups. Their sulfur atoms participate in strongly distorted tetrahedral $Hg^{II}S_3N$ coordination sites. The dimeric building blocks $\{[Hg^{II}(SCN)_3]_2(\mu\text{-}4,4'\text{-bipy})\}$ link consecutive Fe(4,4′-bipy) units. At 220 K, all Fe^{II} sites are crystallographically equivalent. The average Fe–N bond length (2.158(3) Å) is typical of the HS state, in agreement with magnetic data. At 90 K, all Fe^{II} sites are also crystallographically equivalent in a similar ($\boldsymbol{a}$ $\boldsymbol{b}$ $\boldsymbol{c}$) cell and Fe–N (1.962(3) Å) is typical of the LS state (Supporting Information, Tables S1 and S4). The Fe–N bond contraction contributes strongly to the lattice deformation in these polymeric SCO materials.[2f]

A symmetry breaking occurs on the 108–125 K plateau, which corresponds to a doubling along ($\boldsymbol{a}+\boldsymbol{b}+\boldsymbol{c}$) and is characterized by the appearance of superstructure Bragg peaks at $\boldsymbol{Q}_c=\frac{1}{2}\boldsymbol{a}^*+\frac{1}{2}\boldsymbol{b}^*+\frac{1}{2}\boldsymbol{c}^*$ (Supporting Information, Figure S1). The intensity of the Bragg peaks is dependent on temperature (Figure 3c) indicating that this phase is surrounded by two first-order phase transitions around 125 and 108 K, in agreement with magnetic data. The structural refinement at 117 K (Supporting Information, Tables S2 and S4) in the doubled cell reveals two different iron sites: site 1 with Fe1–N ≈ 1.962(3) Å is mainly LS, and site 2 with Fe2–N ≈ 2.146(3) Å is mainly HS. The HS fraction on each site can be estimated from its linear variation with Fe–N.[12] We estimated (Supporting Information, Table S5) $\gamma_{HS}\approx 0.05$ on site 1 and $\gamma_{HS}\approx 0.95$ on site 2. Therefore, the crystal structure consists mainly of HS and LS stripes alternating in a HS-LS-HS-LS sequence along $\boldsymbol{Q}_c$, which can be described as a spin-state concentration wave (SSCW),[8b] and is commensurate with the initial ($\boldsymbol{a}$,$\boldsymbol{b}$,$\boldsymbol{c}$) lattice (Figure 4a). It corresponds to the + − + − + − sequence on the 1/2 step of the Devil's staircase in Figure 2. This spatial modulation of $\gamma_{HS}(\boldsymbol{r})$, translating through the modulation of Fe–N, is schematically represented by a wave in Figure 4a, and is related to the modulation of the probability that crystalline sites in $\boldsymbol{r}$ will be HS:

$$\gamma_{HS}{}^{c}(\mathrm{r}) = \gamma_{HS}{}^{c} + (\eta^{c}/2)\cos(\boldsymbol{Q}_c\,\boldsymbol{r}). \quad (1)$$

It is possible to estimate $\gamma_{HS}{}^{c}\approx 0.5$ from Fe–N = 2.058 Å averaged between sites 1 and 2 (Supporting Information, Table S5), in agreement with magnetic data. The amplitude of the wave is $\eta^{c}\approx 0.9$, which is related to the probability of HS state population by sites 1 or 2. In the ANNNI model,[9d] the 1/2 step is the largest (Figure 2) and consequently the most

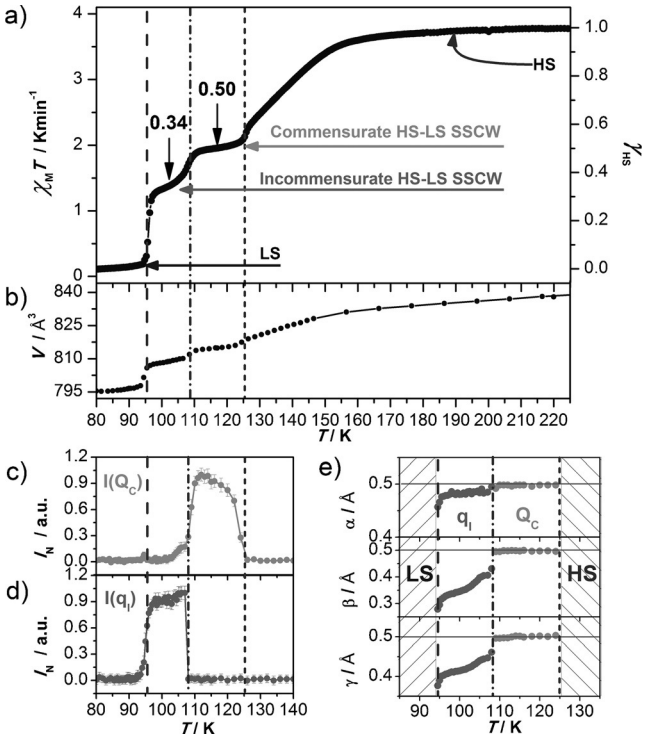

Figure 3. a) Temperature dependence of $\chi_M T$, scaled to γ_{HS}, measured at a 1 $K\,min^{-1}$ cooling rate. b) Unit cell volume given in the ($\boldsymbol{a}$,$\boldsymbol{b}$,$\boldsymbol{c}$) cell of the HS and LS phases. c) Intensity of superstructure peaks indexed $\boldsymbol{Q}_c=\frac{1}{2}\boldsymbol{a}^*+\frac{1}{2}\boldsymbol{b}^*+\frac{1}{2}\boldsymbol{c}^*$ in the HS $\boldsymbol{a}^*$, $\boldsymbol{b}^*$, $\boldsymbol{c}^*$ lattice. d) Intensity of the satellite reflections, indexed $\boldsymbol{q}_i\approx\alpha\boldsymbol{a}^*+\beta\boldsymbol{b}^*+\gamma\boldsymbol{c}^*$. e) Evolution of the coordinates α, β, and γ of $\boldsymbol{Q}_c$ and $\boldsymbol{q}_i$.

© 2016 Wiley-VCH Verlag GmbH & Co. KGaA, Weinheim

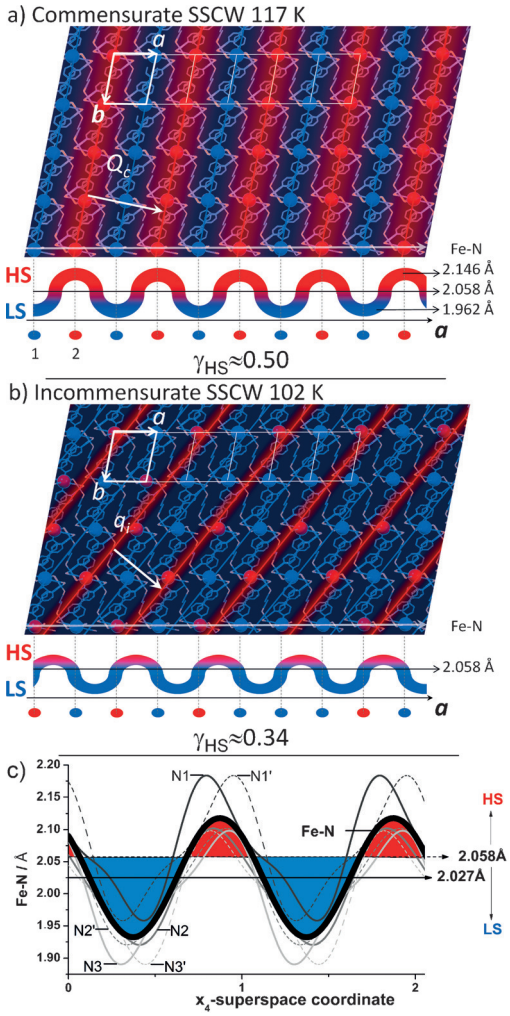

Figure 4. a) Striped structure sliced in the (***a***,***b***) plane of the SSCW forming along $\boldsymbol{Q}_c$. It is commensurate with the (***a***,***b***,***c***) lattice (white) and made of mainly LS (blue, Fe–N = 1.962 Å) and HS (red, Fe–N = 2.146 Å) sites alternating in the LS-HS-LS-HS sequence around Fe–N = 2.058 Å ($\gamma_{HS}^{c} \approx 0.5$). b) Slice in the (***a***,***b***) plane of the aperiodic projected structure, forming an incommensurate SSCW with HS and LS stripes along $\boldsymbol{q}_i$ (projected). c) Modulation of the Fe–N bonds along the superspace coordinate x_4 with an almost sinusoidal modulation of Fe–N (thick line) around ca. 2.027 Å corresponding to $\gamma_{HS}^{i} \approx 0.34$. The fraction of the Fe–N modulation larger than ca. 2.058 Å corresponding primarily to the HS state is also close to $\gamma_{HS}^{i} \approx 0.34$. The schematic waves at the bottom of (a) and (b) show a slice of the spatial HS/LS modulation along the ***a*** axis (white lines at the bottom of the structures).

likely to be observed: HS-LS-HS-LS or HS-HS-LS-LS sequences were reported in different SCO materials.[3,8] Other steps at $\gamma_{HS} = 1/3$ (LS-LS-HS) or $\gamma_{HS} = 2/3$ (HS-HS-LS) are also reported and characterized by a unit cell tripling.[13] The relative stability of the steps is governed by the subtle balance of the interactions and temperature, and for that reason only a limited number of rational steps have been reported experimentally in SCO materials, including 1/4 and 3/4.[3–8,14] Given that another step is observed at $\gamma_{HS} \approx 0.34$, which is close to 1/3, the nature of the order on this step is compelling. The symmetry breaking on the 96–108 K step does not correspond to a unit cell tripling. Different types of Bragg peaks appear, which cannot be indexed with the three vectors basis of the reciprocal lattice (Supporting Information, Figure S1). A fourth vector $\boldsymbol{q}_i$ is required for indexing the scattering vector $\boldsymbol{Q}$ of the peaks, where:

$$\boldsymbol{Q} = h\boldsymbol{a}^* + k\boldsymbol{b}^* + l\boldsymbol{c}^* + m\boldsymbol{q}_i \text{ (h, k, l and m } \in \text{ N), and} \quad (2)$$

$$\boldsymbol{q}_i = \alpha\boldsymbol{a}^* + \beta\boldsymbol{b}^* + \gamma\boldsymbol{c}^*. \quad (3)$$

At 102 K $\alpha \approx 0.48(1)$, $\beta \approx 0.35(1)$, and $\gamma \approx 0.42(1)$ cannot be expressed as simple fractions. The structure is therefore no longer 3D periodic, but incommensurately modulated with respect to the initial (***a***,***b***,***c***) lattice.[15,16] It belongs to the 4D superspace group $P\bar{1}(\alpha,\beta,\gamma)0$ (SSG number 2.1.1.1).[17] Discontinuous changes to the intensities of satellites around 96 and 108 K (Figure 3 d), concomitant with $\chi_M T$ and V jumps, underline the first-order nature of the transitions delimiting the stability region of the incommensurate phase. This incommensurate structure was refined in a (3 + 1)-dimensional superspace[15] (Supporting Information, Table S3), where atomic coordinates are described by their positions in the average 3D unit cell, plus the modulation functions of these coordinates along the fourth dimension coordinate x_4 (Supporting Information, Figure S2), consequently modulating the Fe–N bond distances (Figure 4 c). The in-phase modulation of these bonds along x_4 is the direct proof of the formation of a SSCW along $\boldsymbol{q}_i$, incommensurate with the average 3D periodic crystal lattice, as observed in another SCO material.[16] The average modulation of the six Fe–N bonds indicates an almost sinusoidal modulation function of γ_{HS}: $\gamma_{HS}^{i}(\boldsymbol{r}) = \gamma_{HS}^{i} + (\eta^i/2)\cos(\boldsymbol{q}_i\boldsymbol{r})$ (Figure 4 c), where $\gamma_{HS}^{i} = 0.34$ and $\eta^i = 0.85$ (Supporting Information, Tables S4 and S5). The HS fraction modulation along x_4, with Fe–N > 2.058 Å, fits with $\gamma_{HS}^{i} = 0.34$. The modulation vector $\boldsymbol{q}_i$ of $\gamma_{HS}^{i}(\boldsymbol{r})$, forming HS and LS stripes, is incommensurate with the (***a***,***b***,***c***) lattice. This 4D structure can then be projected in the physical 3D space to reveal the aperiodic spatial distribution of LS and HS states (Figure 4 b).

In the case of a theoretical Devil's staircase, the conversion from $\gamma_{HS} = 1$ to $\gamma_{HS} = 0$ can occur through every rational value n/m (Figure 2). Raising the question: does this $\gamma_{HS}^{i} = 0.34$ step really correspond to an incommensurate phase, or is it simply a high order n/m commensurate phase? On this step, $\boldsymbol{q}_i$ and γ_{HS} continuously change (Figure 3 e) and the SSCW is therefore not locked at a commensurate position of the lattice. This behavior is characteristic of incommensurate structures,[15,16] contrary to the commensurate step $\gamma_{HS} = 1/2$ where $\boldsymbol{Q}_c$ is locked at $\boldsymbol{Q}_c = \frac{1}{2}\boldsymbol{a}^* + \frac{1}{2}\boldsymbol{b}^* + \frac{1}{2}\boldsymbol{c}^*$ from 108 to 125 K.

This study can be viewed as a first step towards a Devil's staircase SCO phenomenon, from the fully HS ($\gamma_{HS} = 1$) to LS ($\gamma_{HS} = 0$) phases, with two long-range ordered structures on the steps: 1) a commensurate SSCW with $\gamma_{HS} \approx 0.5$ and a locked modulation vector $\boldsymbol{Q}_c$ generating a HS-LS-HS-LS sequence; 2) an incommensurate SSCW with $\gamma_{HS} \approx 0.34$ and with a modulation vector slightly evolving around $\boldsymbol{q}_i = 0.48\boldsymbol{a}^* + 0.35\boldsymbol{b}^* + 0.42\boldsymbol{c}^*$.

© 2016 Wiley-VCH Verlag GmbH & Co. KGaA, Weinheim

A true Devil's staircase involves many transitions, in which the wave vector changes by a small amount and is commensurate at each step. The present multi-step process corresponds to an incomplete Devil's staircase as an incommensurate phase forms,[9c] and proves that the most stable phases are not always 3D periodic. The SSCW concept in Figure 2 and 4 can be used to describe the different commensurate steps observed in different SCO crystals.[3–6,13,14] It shows basic features similar to charge density, spin density, or atomic concentration waves,[10] but the present electronic order is unusual because it is related to entropy-driven molecular magnetic bistability.

Acknowledgements

This work was supported by the Spanish Ministerio de Economia *y* Competitividad (MINECO), FEDER (CTQ2013-46275-P), Unidad de Excelencia María de Maeztu MDM-2015-0538, the Generalitat Valenciana through PROMETEO/2012/049. L.P.L. and F.J.V.M. thank the Universidad de Valencia and a MINECO for a predoctoral (FPI) grant. D.Z. thanks the Natural Science Foundation of China and China Scholarship Council. This work was supported by the Institut Universitaire de France, the National Research Agency (ANR-13-BS04-0002), Rennes Metropole and CNRS (Post-Doc funding of E.T.). E.C. and J.A.R. would like to thank G. Chastanet for meditations on the Devil's staircase.

Keywords: aperiodicity · coordination polymers · Devil's staircase · phase transitions · spin-crossover

How to cite: *Angew. Chem. Int. Ed.* **2016**, *55*, 8675–8679
Angew. Chem. **2016**, *128*, 8817–8821

[1] *Spin-crossover materials* (Ed.: M. Halcrow), Wiley, Chichester, **2013**, ISBN 9781119998679.

[2] a) P. Chakraborty, C. Enachescu, A. Humair, L. Egger, T. Delgado, A. Tissot, L. Guénée, C. Besnard, R. Bronisz, A. Hauser, *Dalton Trans.* **2014**, *43*, 17786–17796; b) M. Buron-Le Cointe, J. Hébert, C. Baldé, N. Moisan, L. Toupet, P. Guionneau, J.-F. Létard, E. Freysz, H. Cailleau, E. Collet, *Phys. Rev. B* **2012**, *85*, 064114; c) C. Lochenie, W. Bauer, A. P. Railliet, S. Schlamp, Y. Garcia, B. Weber, *Inorg. Chem.* **2014**, *53*, 11563–11572; d) A. Tissot, R. Bertoni, E. Collet, L. Toupet, M. L. Boillot, *J. Mater. Chem.* **2011**, *21*, 18347–18353; e) B. Weber, W. Bauer, J. Obel, *Angew. Chem. Int. Ed.* **2008**, *47*, 10098–10101; *Angew. Chem.* **2008**, *120*, 10252–10255; f) E. Collet, L. Henry, L. Piñeiro-López, L. Toupet, J. A. Real, *Curr. Inorg. Chem.* **2016**, *6*, 61–66; g) R. Bertoni, M. Lorenc, H. Cailleau, A. Tissot, J. Laisney, M.-L. Boillot, L. Stoleriu, A. Stancu, C. Enachescu, E. Collet, *Nat. Mater.* **2016**, DOI: 10.1038/nmat4606.

[3] a) D. Chernyshov, M. Hostettler, K. W. Törnroos, H.-B. Bürgi, *Angew. Chem. Int. Ed.* **2003**, *42*, 3825–3830; *Angew. Chem.* **2003**, *115*, 3955–3960; b) S. Bonnet, G. Molnár, C. J. Sánchez, M. A. Siegler, A. L. Spek, A. Bousseksou, W.-T. Fu, P. Gamez, J. Reedijk, *Chem. Mater.* **2009**, *21*, 1123–1136; c) N. Bréfuel, H. Watanabe, L. Toupet, J. Come, N. Matsumoto, E. Collet, K. Tanaka, J.-P. Tuchagues, *Angew. Chem. Int. Ed.* **2009**, *48*, 9304–9307; *Angew. Chem.* **2009**, *121*, 9468–9471; d) N. Bréfuel, E. Collet, H. Watanabe, M. Kojima, N. Matsumoto, L. Toupet, K. Tanaka, J.-P. Tuchagues, *Chem. Eur. J.* **2010**, *16*, 14060–14068; e) S. Bonnet, M. A. Siegler, J. S. Costa, G. Molnár, A. Bousseksou, A. L. Spek, P. Gamez, J. Reedijk, *Chem. Commun.* **2008**, 5619–5621; f) M. Buron-Le Cointe, N. Ould Moussa, E. Trzop, A. Moréac, G. Molnár, L. Toupet, A. Bousseksou, J.-F. Létard, G. S. Matouzenko, *Phys. Rev. B* **2010**, *82*, 214106; g) K. Nakano, S. Kawata, K. Yoneda, A. Fuyuhiro, T. Yagi, S. Nasu, S. Morimoto, S. Kaizaki, *Chem. Commun.* **2004**, 2892–2893; h) D. L. Reger, C. A. Little, V. G. Young, Jr., M. Pink, *Inorg. Chem.* **2001**, *40*, 2870–2874; i) T. Sato, K. Nishi, S. Iijima, M. Kojima, N. Matsumoto, *Inorg. Chem.* **2009**, *48*, 7211–7229; j) M. Yamada, H. Hagiwara, H. Torigoe, N. Matsumoto, M. Kojima, F. Dahan, J.-P. Tuchagues, N. Re, S. Iijima, *Chem. Eur. J.* **2006**, *12*, 4536–4549; k) K. W. Törnroos, M. Hostettler, D. Chernyshov, B. Vangdal, H.-B. Bürgi, *Chem. Eur. J.* **2006**, *12*, 6207–6215; l) V. A. Money, C. Carbonera, J. Elhaiek, M. A. Halcrow, J. A. K. Howard, J.-F. Létard, *Chem. Eur. J.* **2007**, *13*, 5503–5514; m) J. Kusz, M. Nowak, P. Gütlich, *Eur. J. Inorg. Chem.* **2013**, 832–842; n) W. Hibbs, P. J. van Koningsbruggen, A. M. Arif, W. W. Shum, J. S. Miller, *Inorg. Chem.* **2003**, *42*, 5645–5653; o) A. Lennartson, A. D. Bond, S. Piligkos, C. J. McKenzie, *Angew. Chem. Int. Ed.* **2012**, *51*, 11049–11052; *Angew. Chem.* **2012**, *124*, 11211–11214; p) M. Nihei, H. Tahira, N. Takahashi, Y. Otake, Y. Yamamura, K. Saito, H. Oshio, *J. Am. Chem. Soc.* **2010**, *132*, 3553–3560; q) G. Agustí, M. C. Muñoz, A. B. Gaspar, J. A. Real, *Inorg. Chem.* **2008**, *47*, 2552–2561; r) T. Kosone, C. Kanadani, T. Saito, T. Kitazawa, *Polyhedron* **2009**, *28*, 1930–1934; s) J. B. Lin, W. Xue, B. Y. Wang, J. Tao, W. X. Zhang, J. P. Zhang, X. M. Chen, *Inorg. Chem.* **2012**, *51*, 9423–9430; t) C. J. Adams, M. C. Muñoz, R. E. Waddington, J. A. Real, *Inorg. Chem.* **2011**, *50*, 10633–10642; u) V. Martínez, A. B. Gaspar, M. Carmen Munoz, G. V. Bukin, G. Levchenko, A. Real, *Chem. Eur. J.* **2009**, *15*, 10960–10971; v) G. Agustí, A. B. Gaspar, M. C. Muñoz, J. A. Real, *Inorg. Chem.* **2007**, *46*, 9646–9654.

[4] a) B. J. C. Vieira, J. T. Coutinho, I. C. Santos, L. C. J. Pereira, J. C. Waerenborgh, V. da Gama, *Inorg. Chem.* **2013**, *52*, 3845–3850; b) M. Griffin, S. Shakespeare, H. J. Shepherd, C. J. Harding, J.-F. Létard, C. Desplanches, A. E. Goeta, J. A. K. Howard, A. K. Powell, V. Mereacre, Y. Garcia, A. D. Naik, H. Müller-Bunz, G. G. Morgan, *Angew. Chem. Int. Ed.* **2011**, *50*, 896–900; *Angew. Chem.* **2011**, *123*, 926–930; c) Z.-Y. Li, J.-W. Dai, Y. Shiota, K. Yoshizawa, S. Kanegawa, O. Sato, *Chem. Eur. J.* **2013**, *19*, 12948–12952; d) K. D. Murnaghan, C. Carbonera, L. Toupet, M. Griffin, M. M. Dîrtu, C. Desplanches, Y. Garcia, E. Collet, J.-F. Létard, G. G. Morgan, *Chem. Eur. J.* **2014**, *20*, 5613–5618; e) D. J. Harding, W. Phonsri, P. Harding, K. S. Murray, B. Moubaraki, G. N. L. Jameson, *Dalton Trans.* **2015**, *44*, 15079–15082.

[5] a) M. G. Cowan, J. Olguín, S. Narayanaswamy, J. L. Tallon, S. Brooker, *J. Am. Chem. Soc.* **2012**, *134*, 2892–2894; b) S. Hayami, Y. Komatsu, T. Shimizu, H. Kamihata, Y. H. Lee, *Coord. Chem. Rev.* **2011**, *255*, 1981–1990; c) S. Hayami, K. Murata, D. Urakami, Y. Kojima, M. Akita, K. Inoue, *Chem. Commun.* **2008**, 6510–6512; d) S. Hayami, Y. Shigeyoshi, M. Akita, K. Inoue, K. Kato, K. Osaka, M. Takata, R. Kawajiri, T. Mitani, Y. Maeda, *Angew. Chem. Int. Ed.* **2005**, *44*, 4899–4903; *Angew. Chem.* **2005**, *117*, 4977–4981.

[6] A. J. Fitzpatrick, E. Trzop, E. Müller-Bunz, M. Dîrtu, Y. Garcia, E. Collet, G. G. Morgan, *Chem. Commun.* **2015**, *51*, 17540–17543.

[7] a) A. Bousseksou, F. Varret, J. Nasser, *J. Phys. I* **1993**, *3*, 1463–1473; b) D. Chernyshov, H.-B. Burgi, M. Hostettler, K. W. Törnroos, *Phys. Rev. B* **2004**, *70*, 094116; c) M. Nishino, K. Boukheddaden, S. Miyashita, F. Varret, *Phys. Rev. B* **2003**, *68*, 224402.

 © 2016 Wiley-VCH Verlag GmbH & Co. KGaA, Weinheim

[8] a) K. Boukheddaden, J. Linares, R. Tanasa, C. Chong, *J. Phys. Condens. Matter* **2007**, *19*, 106201; b) H. Watanabe, K. Tanaka, N. Bréfuel, H. Cailleau, J.-F. Létard, S. Ravy, P. Fertey, M. Nishino, S. Miyashita, E. Collet, *Phys. Rev. B* **2016**, *93*, 014419.

[9] a) P. Bak, J. von Boehm, *Phys. Rev.* **1980**, *21*, 5297; b) M. E. Fisher, W. Selke, *Phys. Rev. Lett.* **1980**, *44*, 1502; c) S. Aubry, *J. Physique* **1983**, *44*, 147 – 162; d) P. Bak, R. Bruinsma, *Phys. Rev. Lett.* **1982**, *49*, 249 – 251.

[10] a) M. Gao, C. Lu, H. Jean-Ruel, L. C. Liu, A. Marx, K. Onda, S. Koshihara, Y. Nakano, X. Shao, T. Hiramatsu, G. Saito, H. Yamochi, R. R. Cooney, G. Moriena, G. Sciaini, R. J. D. Miller, *Nature* **2013**, *496*, 343 – 346; b) P. Monceau, *Adv. Phys.* **2012**, *61*, 325 – 581; c) K. Ohwada, Y. Fujii, N. Takesue, M. Isobe, Y. Ueda, H. Nakao, Y. Wakabayashi, Y. Murakami, K. Ito, Y. Amemiya, H. Fujihisa, K. Aoki, T. Shobu, Y. Noda, N. Ikeda, *Phys. Rev. Lett.* **2001**, *87*, 086402; d) K. Machida, M. Nakano, *J. Phys. Soc. Jpn.* **1990**, *59*, 4223 – 4226; e) A. Murakami, Y. Tsunoda, *Phys. Rev. B* **2000**, *61*, 5998; f) M. Hupalo, J. Schmalian, M. C. Tringides, *Phys. Rev. Lett.* **2003**, *90*, 216106; g) T. Isozaki, T. Fujikawa, H. Takezoe, A. Fukuda, T. Hagiwara, Y. Suzuki, I. Kawamura, *Phys. Rev. B* **1993**, *48*, 13439 – 13450; h) T. Matsuda, S. Partzsch, T. Tsuyama, E. Schierle, E. Weschke, J. Geck, T. Saito, S. Ishiwata, Y. Tokura, H. Wadati, *Phys. Rev. Lett.* **2015**, *114*, 236403.

[11] Details on crystallographic data for the bimetallic 2D coordination polymer at 220 K (CCDC-1457783), 90 K (CCDC-1457781), 117 K (CCDC-1457782), and 102 K (CCDC-1457785) can be found in the Supporting Information. CCDC 1457783, 1457781, 1457782, and 1457785 contain the supplementary crystallographic data for this paper. These data can be obtained free of charge from The Cambridge Crystallographic Data Centre.

[12] E. Collet, M. L. Boillot, J. Hébert, N. Moisan, M. Servol, M. Lorenc, L. Toupet, M. Buron-Le Cointe, A. Tissot, J. Sainton, *Acta Crystallogr. Sect. B* **2009**, *65*, 474 – 480.

[13] a) S. Pillet, E. E. Bendeif, S. Bonnet, H. J. Shepherd, P. Guionneau, *Phys. Rev. B* **2012**, *86*, 064106; b) J. Luan, J. Zhou, Z. Liu, B. Zhu, H. Wang, X. Bao, W. Liu, M.-L. Tong, G. Peng, H. Peng, L. Salmon, A. Bousseksou, *Inorg. Chem.* **2015**, *54*, 5145 – 5147; c) G. Agustí, A. B. Gaspar, M. C. Muñoz, P. Lacroix, J. A. Real, *Aust. J. Chem.* **2009**, *62*, 1155 – 1165; d) Z.-Y. Li, H. Ohtsu, T. Kojima, J.-W. Dai, T. Yoshida, B. K. Breedlove, W.-X. Zhang, H. Iguchi, O. Sato, M. Kawano, M. Yamashita, *Angew. Chem. Int. Ed.* **2016**, *55*, 5184 – 5189; *Angew. Chem.* **2016**, *128*, 5270 – 5275.

[14] a) N. F. Sciortino, K. R. Scherl-Gruenwald, G. Chastanet, G. J. Halder, K. W. Chapman, J.-F. Létard, C. J. Kepert, *Angew. Chem. Int. Ed.* **2012**, *51*, 10154 – 10158; *Angew. Chem.* **2012**, *124*, 10301 – 10305; b) N. Bréfuel, E. Collet, H. Watanabe, M. Kojima, N. Matsumoto, L. Toupet, K. Tanaka, J.-P. Tuchagues, *Chem. Eur. J.* **2010**, *16*, 14060 – 14068.

[15] a) T. Janssen, G. Chapuis, M. de Boissieu, *Aperiodic Crystals: From Modulated Phases to Quasicrystals*, Oxford University Press, Oxford, **2007**; b) S. van Smaalen, *Incommensurate Crystallography*, Oxford University Press, Oxford, **2007**; c) A. Janner, T. Janssen, J. C. Toledano, *Lect. Notes Phys.* **1984**, *201*, 364 – 396.

[16] E. Collet, H. Watanabe, N. Bréfuel, L. Palatinus, L. Roudaut, L. Toupet, K. Tanaka, J. P. Tuchagues, P. Fertey, S. Ravy, B. Toudic, H. Cailleau, *Phys. Rev. Lett.* **2012**, *109*, 257206.

[17] H. T. Stokes, B. J. Campbell, S. van Smaalen, *Acta Crystallogr. Sect. A* **2011**, *67*, 45 – 55.

Received: March 9, 2016
Published online: May 19, 2016

 © 2016 Wiley-VCH Verlag GmbH & Co. KGaA, Weinheim